

Nonvolatile bistable memory and Ising machine based on Micro-Electro-Mechanical Systems

Motohiko Ezawa¹, Eric Lebrasseur² and Yoshio Mita²

¹*Department of Applied Physics, University of Tokyo, Hongo 7-3-1, 113-8656, Japan and*

²*Department of Electrical Engineering, University of Tokyo, Hongo 7-3-1, 113-8656, Japan*

We propose nonvolatile binary stable states based on microelectromechanical systems (MEMS). They may be used as MEMS memory, where the bistable memory is the buckling direction of a plate of a capacitor. The binary memory is switched by applying a voltage to the MEMS. Furthermore, we propose an Ising model by making a series of buckled MEMS. It is a great merit of this mechanism that the annealing process is automatically carried out due to the damping effect of the spring. We find a duality relation between the parallel-plate MEMS under constant-voltage condition and the comb-teeth MEMS under constant-charge condition.

I. INTRODUCTION

Many binary-combinatorial problems are described by the Ising model¹. It is called an Ising machine, where a ground state is efficiently obtained by an annealing method. There are various ways for the annealing process. A classical way is a simulated annealing^{2,3}, where we decrease temperature to obtain a ground state. The quantum annealing machine⁴⁻⁶ is one of the most successful quantum machines on a commercial basis although it is not a universal quantum computer. It determines a ground state of a transverse magnetic field Ising model by gradually decreasing the magnetic field.

Recently, many variations of the Ising machine are proposed such as a coherent Ising machine⁷⁻¹¹ based on photonic systems, a simulated bifurcation machine^{12,13} based on digital computer and a probabilistic-bit (p-bit) machine¹⁴⁻¹⁸ based on magnetic systems. The key point is how to make a binary stable state representing the Ising degree of freedom and how to control it. Actually, it is not necessary to be a quantum system to solve this Ising problem. It is advantageous if it is possible to construct an Ising machine with the use of current electric technologies.

A microelectromechanical system (MEMS) is a combinatorial system of electric circuits and mechanical systems^{19,20}. A typical example is an electrostatic actuator consisting of capacitors and springs, which we call a parallel-plate MEMS. Another important MEMS is a comb-teeth electrostatic actuator, which we call a comb-teeth MEMS. In both of these, the capacitance is controlled by tuning the position of plates in the capacitors. Topological physics in MEMS has been discussed^{21,22}.

In this paper, we propose a nonvolatile binary stable state made of a MEMS by buckling plates of capacitors. It may be used as a binary memory. Furthermore, we propose an Ising machine made of the parallel-plate MEMS by controlling the voltage. We also study an Ising machine based on the comb-teeth MEMS by controlling the charge. In the present mechanism, the annealing process is automatically executed due to the damping of the spring. It is highly contrasted to the simulated annealing and the quantum annealing, where it is necessary to precisely control external parameters. It is intriguing that a duality relation holds between the parallel-plate MEMS under constant-voltage condition and the comb-teeth MEMS under constant-charge condition.

This paper is composed as follows. In Sec.II we intro-

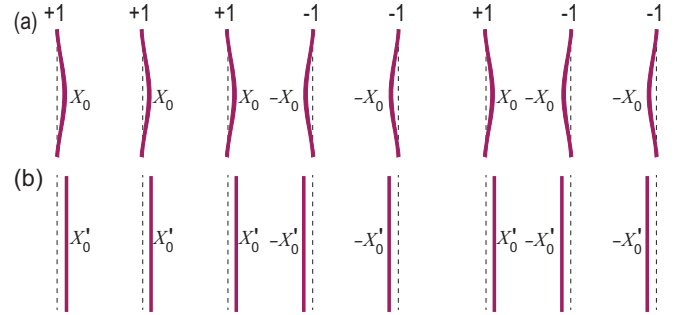


FIG. 1: (a) Illustration of a sequence of buckled MEMS. (b) Effective model of buckled MEMS.

duce a buckled MEMS made of three parallel plates, which is shown to have two stable positions. In Sec.III, we propose a MEMS memory based on this buckled MEMS by imposing the constant-voltage condition. In Sec.IV, we realize an Ising model by placing parallel plates sequentially under the constant-voltage condition. We point out that it fails under the constant-charge condition. In Sec. VI, we realize an Ising model with the use of comb-teeth MEMS under the constant-charge condition. We also point out that it fails under the constant-voltage condition. We summarize these results on the MEMS Ising model in a table:

	Parallel plate	Comb teeth
Constant voltage	○	×
Constant charge	×	○

Sec. VII is devoted to discussion.

II. BUCKLED MEMS

We consider a system made of N plates placed parallelly with equal separation. We push a plate from both edges to buckled it. There are two stable positions, as shown in Fig.1(a). Its energy is well approximated by

$$U_{\text{spring}} = \sum_{j=1}^N \frac{\alpha}{2} (u_j^2 - X_0^2)^2, \quad (1)$$

where α is the strength of the potential and u_j is the position of the j -th plate at $y = 0$. The local minima of the potential

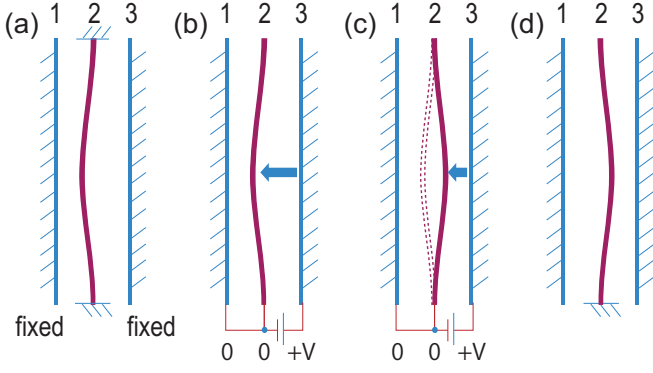


FIG. 2: Flip process of the MEMS memory. (a) The initial position of the plate is $u = -X_0$. (b) We apply voltage between the central and the right plates. (c) The position is flipped from $u = -X_0$ to $u = X_0$. (d) We remove the voltage, where the plate is fixed at $u = X_0$.

are given by

$$u_j = \pm X_0. \quad (2)$$

The potential barrier is given by

$$U_0 = \frac{\alpha}{2} X_0^4 \equiv \frac{\kappa \ell^2}{2}, \quad (3)$$

where κ is the spring constant of the plate and ℓ is the amount of the length which is shortened by buckling. Hence, we obtain $\alpha = \kappa \ell^2 / X_0^4$.

We may approximate a buckled plate by a straight plate with displacement X'_0 as shown in Fig.1(b). Here, X'_0 is a quantity in the order of X_0 . For brevity we use the potential (1) with u_j and X_0 as the quantities for the straight plane in the effective theory in what follows.

With this approximation, the capacitance between the plate u_j and u_{j+1} is well described by

$$C_{\text{para}}(u_j, u_{j+1}) = \frac{\varepsilon_0 S}{X_{\text{cap}} + u_j - u_{j+1}}, \quad (4)$$

where X_{cap} is the distance between the neighboring plates without buckling, S is the area of the plate, and ε_0 is the permittivity.

The electrostatic potential is given by

$$U_{\text{cap}} = \sum_{j=1}^{N-1} \frac{C_{\text{para}}(u_j, u_{j+1})}{2} V_j^2, \quad (5)$$

when we control the voltage. On the other hand, it is given by

$$U_{\text{cap}} = \sum_{j=1}^{N-1} \frac{Q_j^2}{2C_{\text{para}}(u_j, u_{j+1})}, \quad (6)$$

when we control the charge.

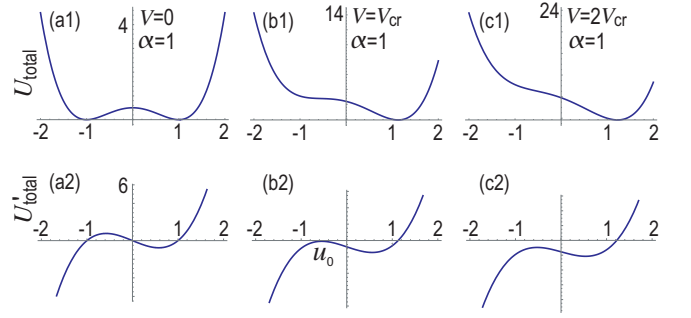


FIG. 3: (a1) Total potential U_{total} with $V = 0$ (i.e., the spring potential U_{spring}) for three plates given by Fig.2, where $u_1 = u_3 = 0$. (b1) U_{total} with $V = V_{\text{cr}}$. (c1) U_{total} with $V > V_{\text{cr}}$. (a2), (b2) and (c2) corresponding differential of the potential $U'_{\text{total}} = \partial U_{\text{total}} / \partial u$. We have set $\alpha = 1$. The horizontal axis is the position in units of X_0 .

III. MEMS MEMORY

We first consider a system consisting of three plates as shown in Fig.2. The outermost two plates are fixed at the position $u_1 = u_3 = 0$, while the inner plate $u \equiv u_2$ can move freely. There are two stable positions $u = \pm X_0$, which can store a binary information. It can be used as a binary memory.

We discuss how to flip the stored information. We choose the initial state $u = -X_0$, as shown in Fig.2(a). We apply a voltage between the right and middle plates as shown in Fig.2(b). The electrostatic potential is given by

$$C_{\text{para}}(u) = \frac{\varepsilon_0 S}{X_{\text{cap}} + u}. \quad (7)$$

The static energy is given by

$$U_{\text{cap}} = \frac{C_{\text{para}}(u)}{2} V^2, \quad (8)$$

when we apply a constant voltage V between the right and middle plates.

The position u is determined by the total potential,

$$U_{\text{total}}(u) = \frac{\alpha}{2} (u^2 - X_0^2)^2 + \frac{C_{\text{para}}(u)}{2} V^2. \quad (9)$$

We analyze the condition for the central plate to move from the left position to the right position without a barrier: See Fig.2(c) and Fig.3. The condition is that the slope of the curve $U_{\text{total}}(u)$ is negative, $\partial U_{\text{total}} / \partial u < 0$, for all $|u| < X_0$. In order to solve this condition, we determine a position u_0 where the slope of $\partial U_{\text{total}} / \partial u$ is zero, or

$$\left. \frac{\partial^2 U_{\text{total}}}{\partial u^2} \right|_{u_0} = 0. \quad (10)$$

If the condition

$$\left. \frac{\partial U_{\text{total}}}{\partial u} \right|_{u_0} < 0 \quad (11)$$

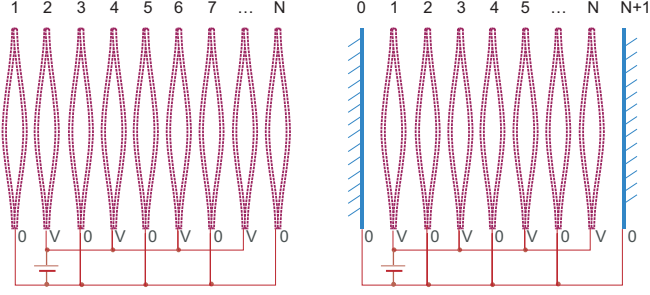


FIG. 4: (a) Free-boundary condition and (b) fixed-boundary condition for a series of buckled MEMS .

is satisfied at this position $u = u_0$, it follows that $\partial U_{\text{total}}/\partial u < 0$ for $u < X_0$. See Fig.3(c2).

Solving Eq.(10) we find $u_0 = -X_0/\sqrt{3}$, where we have used an approximation $X_{\text{cap}} \gg u$. Now, the condition (11) yields $V > V_{\text{cr}}$, with

$$V_{\text{cr}} = \frac{4\alpha X_0^3 X_{\text{cap}}^2}{3\sqrt{3}}. \quad (12)$$

The plate position flip from $u = -X_0$ to $u = X_0$ for $V > V_{\text{cr}}$. Finally, we remove the voltage, where the plate is fixed at $u = X_0$, as shown in Fig.2(d).

The position of the plate can be read out by measuring the capacitance.

IV. ISING MODEL

We next realize the Ising model by considering a series of buckled MEMS as in Fig.4. The potential energy of the buckled MEMS system is given by

$$U_{\text{total}} = U_{\text{spring}} + U_{\text{cap}}, \quad (13)$$

where U_{spring} is given by Eq.(1) and

$$U_{\text{cap}} = \sum_{j=1}^{N-1} \frac{C_{\text{para}}(u_j, u_{j+1})}{2} V_j^2, \quad (14)$$

Provided the applied voltage V_j is sufficiently smaller than V_{cr} , the ground state is given by Eq.(2), or $s_j \equiv u_j/X_0 = \pm 1$. Such a binary system is well described by the Ising model.

The Ising model is given by

$$H_{\text{Ising}} = \sum_{j=1}^{N-1} J_j s_j s_{j+1} + \sum_{j=1}^N B_j s_j + E_0, \quad (15)$$

where the parameters J_j , B_j and E_0 are determined in what follows.

The energy spectrum is given by setting $s_j = \pm 1$. On the other hand, the energy spectrum of the buckled MEMS system H_{MEMS} is given by setting $u_j = X_0 s_j$ provided $V/V_{\text{cr}} \ll 1$. We may identify the energy spectra of these two systems in this case.

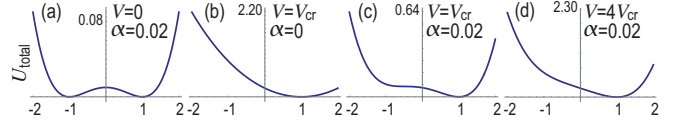


FIG. 5: Total potential energy U_{total} for three neighboring plates in Fig.4, where $u_1 = u_3 = X_0$. (a) Spring potential (1) with $\alpha = 0.02$. (b) Electrostatic potential (8) with $\alpha = 0$ and $V = V_{\text{cr}}$. (c) $\alpha = 0.02$ and $V = V_{\text{cr}}$. (d) $\alpha = 0.02$ and $V = 4V_{\text{cr}}$.

We start with considering a system made of two adjacent plates,

$$H_j(s_j, s_{j+1}) = J_j s_j s_{j+1} + \frac{B_j}{2} s_j + \frac{B_{j+1}}{2} s_{j+1} + \frac{E_0}{N-1}, \quad (16)$$

where

$$H_{\text{Ising}} = \sum_{j=1}^{N-1} H_j(s_j, s_{j+1}) + \frac{B_1}{2} s_1 + \frac{B_N}{2} s_N \quad (17)$$

On the other hand, considering two adjacent plates, we obtain a formula

$$H_j(s_j, s_{j+1}) = \frac{C_{\text{para}}(u_j, u_{j+1})}{2} V_j^2 \quad (18)$$

with $u_j = X_0 s_j$ under the constant-voltage condition. Note that we have $U_{\text{spring}} = 0$ since the plates exist at the stable position.

We write down $H_{j,j+1}(s_j, s_{j+1})$ explicitly,

$$H_j(1, 1) = J_j + B'_j + B'_{j+1} + E'_0 \equiv \mathcal{E}_0, \quad (19)$$

$$H_j(1, -1) = -J_j + B'_j - B'_{j+1} + E'_0 \equiv \mathcal{E}_+, \quad (20)$$

$$H_j(-1, 1) = -J_j - B'_j + B'_{j+1} + E'_0 \equiv \mathcal{E}_-, \quad (21)$$

$$H_j(-1, -1) = J_j - B'_j - B'_{j+1} + E'_0 \equiv \mathcal{E}_0, \quad (22)$$

where we have defined $B'_j = B_j/2$ and $E'_0 = E_0/(N-1)$. It follows from Eqs.(18) and (4) that

$$\mathcal{E}_0 = \frac{\varepsilon_0 S}{X_{\text{cap}} - X_0 + X_0} \frac{V_j^2}{2} = \frac{\varepsilon_0 S}{X_{\text{cap}}} \frac{V_j^2}{2}, \quad (23)$$

$$\mathcal{E}_{\pm} = \frac{\varepsilon_0 S}{X_{\text{cap}} \mp X_0 \mp X_0} \frac{V_j^2}{2} = \frac{\varepsilon_0 S}{X_{\text{cap}} \mp 2X_0} \frac{V_j^2}{2}. \quad (24)$$

We find $\mathcal{E}_+ > \mathcal{E}_0 > \mathcal{E}_-$. Hence, the coefficients in the Ising model are given

$$J_j = \frac{2\mathcal{E}_0 - \mathcal{E}_+ - \mathcal{E}_-}{4} = -\frac{2\varepsilon_0 S V_j^2 X_0^2}{X_{\text{cap}} (X_{\text{cap}}^2 - 4X_0^2)}, \quad (25)$$

$$B_j = -B_{j+1} = \frac{\mathcal{E}_+ - \mathcal{E}_-}{4} = \frac{\varepsilon_0 S V_j^2 X_0}{(X_{\text{cap}}^2 - 4X_0^2)}, \quad (26)$$

$$E_0 = \frac{2\mathcal{E}_0 + \mathcal{E}_+ + \mathcal{E}_-}{4} = \frac{2\varepsilon_0 S V_j^2 (X_{\text{cap}}^2 - X_0^2)}{X_{\text{cap}} (X_{\text{cap}}^2 - 4X_0^2)}, \quad (27)$$

in terms of the quantities of the buckled MEMS system.

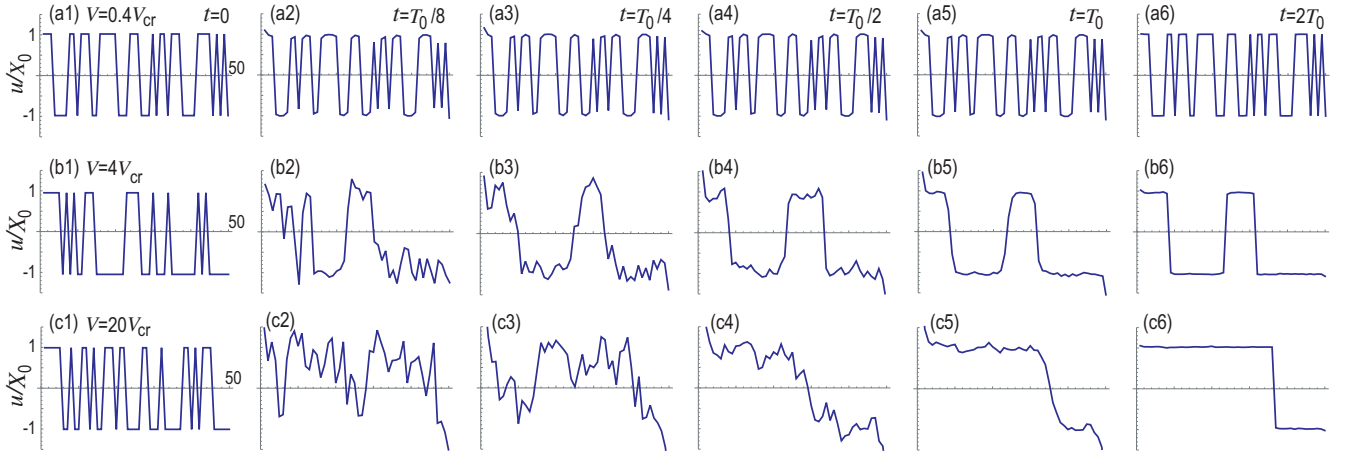


FIG. 6: Dynamics with the free-boundary condition. Configuration u_j/X_0 at (a1)~(c1) the initial state $t = 0$, (a2)~(c2) $t = T_0/8$, (a3)~(c3) $t = T_0/4$, (a4)~(c4) $t = T_0/2$, (a5)~(c5) $t = T_0$ and (a6)~(c6) $t = 2T_0$. We have used a 50-plate system. We have applied voltage (a1)~(a3) $V = 0.4V_{cr}$, (b1)~(b3) $V = 4V_{cr}$ and (c1)~(c3) $V = 20V_{cr}$. (a1)~(a3) There is no annealing when the voltage is below the critical value ($V < V_{cr}$). (b1)~(b3) There remain three domain walls after annealing when the voltage exceeds the critical value but not sufficiently. (c1)~(c3) The annealing process is perfect when the voltage exceeds the critical value sufficiently. The vertical axis is the configuration u_j/X_0 . The horizontal axis is the position j . We have set $\alpha = 0.02$, $\gamma = 0.01$, $T_0 = 500X_0 = 1$.

The generalization to a chain of N plates is straightforward. The Hamiltonian (15) is reduced to

$$H_{\text{Ising}} = \sum_{j=1}^{N-1} J_j s_j s_{j+1} + B_1 s_1 + B_N s_N + E_0, \quad (28)$$

since the $B_j s_j$ terms cancel except for the end plates. Here, J_j , $B_1 = -B_N$ and E_0 are given by Eqs.(25), (26) and (27), respectively.

A. Dynamics

We have shown that a series made of buckled MEMS is well described by the Ising model in the presence of a small external voltage. We start with an initial state, where $s_j = \pm 1$ is randomly assigned to the site i . Although it is not the ground state, the configuration is stable because the plate position cannot be flipped. The buckled MEMS system may serve as an annealing machine, as we now argue.

We study the dynamics of the system, where we explicitly analyze the dynamics of the plate position u_j . The Lagrangian of the system is given by the kinetic term K and the potential (9),

$$L = K - U_{\text{total}}, \quad (29)$$

with

$$K = \sum_j \frac{m}{2} \dot{u}_j^2, \quad (30)$$

where $\dot{u}_j = du_j/dt$ is the velocity of the plate. The Euler-Lagrange equation is

$$\frac{d}{dt} \left(\frac{\partial L}{\partial \dot{u}_j} \right) - \frac{\partial L}{\partial u_j} + \frac{\partial R}{\partial \dot{u}_j} = 0, \quad (31)$$

where we have introduced the Rayleigh dissipation function in order to describe the damping of the spring,

$$R = \sum_j \frac{\gamma}{2} \dot{u}_j^2, \quad (32)$$

with γ being the damping factor. Eq.(31) is explicitly written down as

$$\begin{aligned} \frac{m}{2} \ddot{u}_j^2 + \gamma \dot{u}_j = & -2\beta u_j (u_j^2 - X_0) - \frac{\varepsilon_0 S V_j^2}{(X_{\text{cap}} + u_j - u_{j+1})^2} \\ & + \frac{\varepsilon_0 S V_j^2}{(X_{\text{cap}} + u_{j-1} - u_j)^2}, \end{aligned} \quad (33)$$

which we solve numerically.

The dynamics can be understood intuitively by plotting the energy (13). For simplicity, we first consider three plates, where two outermost plates are fixed at the position $u_1 = u_3 = X_0$ while the inner plate moves freely. The electrostatic potential is given by

$$U_{\text{cap}} = \frac{\varepsilon_0 S}{X_{\text{cap}} - u + X_0} + \frac{\varepsilon_0 S}{X_{\text{cap}} - X_0 + u}. \quad (34)$$

We show the electrostatic potential as a function of the position of the inner plate u in Fig.5(b). It takes a minimum at $u = X_0$, which indicates that the inner plate tends to take the same position as the outermost plates. There are two minima in the spring potential energy as shown in Fig.5(a). By increasing the voltage, the energy balance is broken. Fig.5(c) shows a potential with a critical voltage. Once the voltage exceeds the critical point, the potential has only one minimum without energy barrier as shown in Fig.5(d). Then, the inner plate moves so that the position u is identical to the positions of the outermost plates, i.e., $u = u_1 = u_3 = X_0$. It corresponds to the ferromagnetic interaction in the Ising model.

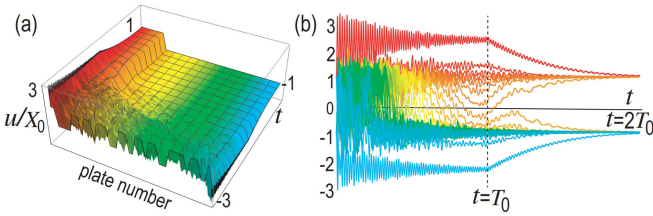


FIG. 7: Time evolution of the annealing process. (a) Bird's eye's view and (b) colored plot for each plate. We have used a 50-plate system. The parameters are the same as in Fig.6(b).

We next consider the N -plate system. We apply voltage V_0 for the $(2n)$ -th plate and 0 for the $(2n + 1)$ -th plate as shown in Fig.4, where the potential difference between two adjacent plates is V_0 . We set an initial state randomly at the two local minima $s_j = \pm 1$. There are two boundary conditions. One is the free-boundary condition, where all of plates flip freely as shown in Fig.4(a). The other is the fixed-boundary condition, where the outmost plates are fixed without buckling as shown in Fig.4(b). We first consider the case where all of the plates flip as shown in Fig.4(a), which is the free-boundary condition. There are a number of domain walls as in Fig.6(a1), (b1) and (c1). When the voltage exceeds the critical value, plates can flip in order to minimize the electrostatic potential. We show the time evolution of the plate position applying a constant voltage $V_j = V_0$ in Fig.7(a). The plate position overcomes the potential barrier (3) of the spring in order to minimize the electrostatic potential (14). The number of domain walls decreases as the time evolves. We keep the constant voltage $V_j = V_0$ for a while ($0 < t < T_0$) so that the flipping of plate positions is over as indicated by a vertical dotted line in Fig.7(b). Here, the position u_j deviates from the local minima (2) in the presence of V_0 due to the contribution of the electrostatic potential (14). See Fig.6.

Then, we gradually decrease the voltage. We show the time evolution of domain walls for three typical values of V_0 in Fig.6 by using the formula

$$V_j = \begin{cases} V_0 & \text{for } t < T_0 \\ V_0 \exp\left[-\frac{t-T_0}{\tau}\right] & \text{for } t \geq T_0 \end{cases}, \quad (35)$$

where τ is the decay rate of the voltage. The position u_j converges to the local minima (2) when V_j becomes small.

First we consider the case with $V_0 < V_{cr}$: See Fig.6(a1)~(a6). Since the voltage is below the critical value, the plates can not flip.

Next we consider the case $V_0 > V_{cr}$ but V_0 is not too large: See Fig.6(b1)~(b6). The number of domain walls in the final state substantially decreases comparing with the initial state although some domain walls exist. The reason that we cannot obtain the exact ground state without domain walls is that the state is trapped to a local minimum, which is a universal feature of the annealing method. Indeed, there are many domain walls in actual ferromagnets.

Finally, when V_0 is large enough, the final state falls into the exact ground state with one domain wall, as shown in Fig.6(c6). The emergence of one domain wall is understood

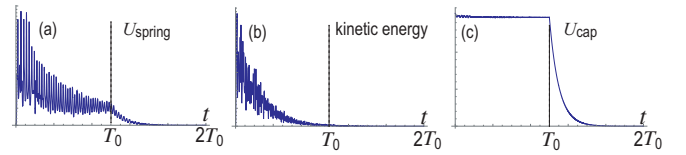


FIG. 8: Time evolution of (a) the spring potential energy U_{spring} , (b) the kinetic energy K , and (c) electrostatic potential U_{cap} . We have used a 16-plate system.

from the form of the Hamiltonian (28). There are "magnetic field" terms B_1 and B_N in both ends, which requires $u_1 = X_0$ and $u_N = -X_0$. The physical meaning is that the outer most plate goes inside in order to minimize the electrostatic potential. In general, the number of the domain walls must be odd.

The damping of the springs plays an essential role in the present annealing process. It is because the total energy automatically decreases due to the damping term. We show the time evolution of the potential of the spring (1) in Fig.8(a). It decreases with oscillations but does not reach the zero energy for $t < T_0$, because the relaxed position deviates from the local minima (2) due to the electrostatic force. After the voltage V_0 becomes sufficiently small for $t \gg T_0$, the potential energy goes to zero. On the other hand, the kinetic energy (30) of the spring decreases to zero even for $T < T_0$ due to the Rayleigh dissipation term (32), as shown in Fig.8(b). Plates flip so that the total energy decreases. This is the annealing process of the present system. It is highly contrasted with the classical and quantum annealing, where it is necessary to gradually decrease temperature or magnetic field due to the lack of dissipation mechanism.

We also show the time evolution of the electrostatic potential in Fig.8(c). It is almost constant for $T < T_0$ and rapidly decreases for $T > T_0$.

Next, we consider the fixed-boundary condition, where the plates at the both sides are fixed without buckling. We show the dynamics in Fig.9. The number of domain walls needs not be odd as shown in Fig.9(b6) and (c6). Especially, we find that the "ferromagnetic" ground state is realized for strong enough voltage as shown in Fig.9(c6). This is because the outermost plates are not necessary to move outside.

We compare the energy of the "ferromagnetic" and the "antiferromagnetic" ground states. The energy of the "ferromagnetic" ground state is

$$U_{\text{cap}}^{\text{F}} = \frac{\varepsilon_0 S}{X_{\text{cap}}} N. \quad (36)$$

On the other hand, the energy of the "antiferromagnetic" ground state is

$$U_{\text{cap}}^{\text{AF}} = \left(\frac{\varepsilon_0 S}{X_{\text{cap}} - X_0} + \frac{\varepsilon_0 S}{X_{\text{cap}} + X_0} \right) \frac{N}{2}. \quad (37)$$

We find $U_{\text{cap}}^{\text{AF}} > U_{\text{cap}}^{\text{F}}$, which implies that the "ferromagnetic" state is preferred.

A comment is in order. We have so far employed the constant-voltage condition. We next examine the parallel

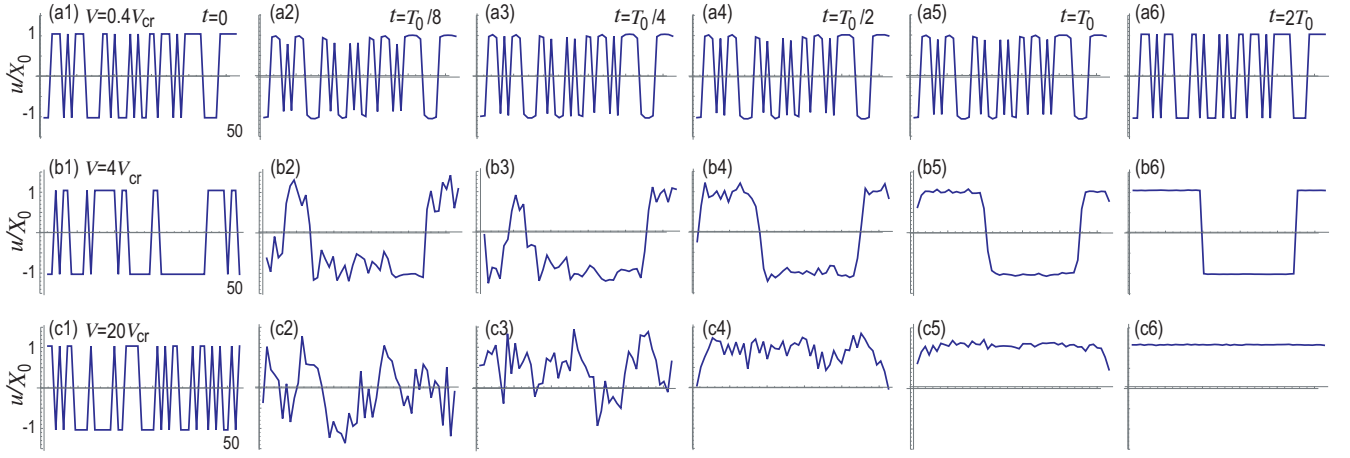


FIG. 9: Dynamics with the fixed-boundary condition. Configuration u_j/X_0 at (a1)~(c1) the initial state $t = 0$, (a2)~(c2) $t = T_0/8$, (a3)~(c3) $t = T_0/4$, (a4)~(c4) $t = T_0/2$, (a5)~(c5) $t = T_0$ and (a6)~(c6) $t = 2T_0$. We have used a 50-plate system. We have applied voltage (a1)~(a3) $V = 0.4V_{cr}$, (b1)~(b3) $V = 4V_{cr}$ and (c1)~(c3) $V = 20V_{cr}$. (a1)~(a3) There is no annealing when the voltage is below the critical value ($V < V_{cr}$). (b1)~(b3) There remain three domain walls after annealing when the voltage exceeds the critical value but not sufficiently enough. (c1)~(c3) The annealing process is perfect when the voltage exceeds the critical value sufficiently. The vertical axis is the configuration u_j/X_0 . The horizontal axis is the position j . We have set $\alpha = 0.02$, $\gamma = 0.01$, $T_0 = 500X_0 = 1$.

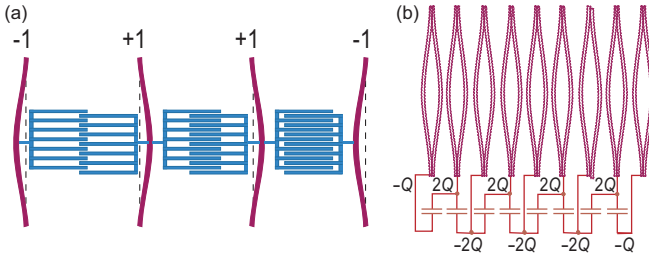


FIG. 10: Illustration of a comb-teeth MEMS combined with buckled plates.

plate system under the constant-charge condition. The static energy is given by

$$U_{\text{cap}} = \sum_j \frac{Q_j^2}{2C_{\text{para}}(u_j, u_{j+1})} = (X_{\text{cap}} + u_j - u_{j+1}) \frac{Q_j^2}{\varepsilon_0 S} \quad (38)$$

in the presence of a constant charge Q_j between the j -th and $(j+1)$ -th plates. We obtain

$$\mathcal{E}_0 = X_{\text{cap}} \frac{Q_j^2}{\varepsilon_0 S}, \quad (39)$$

$$\mathcal{E}_{\pm} = (X_{\text{cap}} \mp 2X_0) \frac{Q_j^2}{\varepsilon_0 S}, \quad (40)$$

instead of Eqs.(23) and (24), and

$$J_j = 0, \quad (41)$$

$$B_j = -B_{j+1} = 4X_0 \frac{Q_j^2}{\varepsilon_0 S}, \quad (42)$$

$$E_0 = \frac{2\mathcal{E}_0 + \mathcal{E}_+ + \mathcal{E}_-}{4} = X_{\text{cap}} \frac{Q_j^2}{\varepsilon_0 S}, \quad (43)$$

instead of Eqs.(25), (26) and (27). These results show that the parallel plate system under the constant-charge condition does not act as the Ising machine.

V. COMB-TEETH MEMS

In the current MEMS technology, comb-teeth electrostatic actuators are mainly used, which we call comb-teeth MEMS. The structure of them are shown in Fig.10(a), where many parallel plates form a comb-teeth like structure. In the comb-teeth MEMS, the capacitance is proportional to the area of the overlap,

$$C_{\text{comb}}(u_j, u_{j+1}) = \frac{\varepsilon_0 d_Y (X_{\text{cap}} + u_j - u_{j+1})}{d_Z}, \quad (44)$$

where d_Z is the distance between the neighboring plates without buckling, and d_Y is the length of the plate along the y direction.

Here we impose the constant-charge condition. The static energy is given by

$$U_{\text{comb}} = \sum_j \frac{Q_j^2}{2C_{\text{comb}}(u_j, u_{j+1})} \quad (45)$$

in the presence of a constant charge Q_j between the j -th and $(j+1)$ -th plates. We consider the configuration shown in Fig.10(a), where the charge difference is Q between the ad-

adjacent plates. It follows that

$$\mathcal{E}_0 = \frac{d_Z}{X_{\text{cap}} - X_0 + X_0} \frac{Q_j^2}{2\varepsilon_0 d_Y} = \frac{d_Z}{X_{\text{cap}}} \frac{Q_j^2}{2\varepsilon_0 d_Y}, \quad (46)$$

$$\mathcal{E}_{\pm} = \frac{d_Z}{X_{\text{cap}} \mp X_0 \mp X_0} \frac{Q_j^2}{2\varepsilon_0 d_Y} = \frac{d_Z}{X_{\text{cap}} \mp 2X_0} \frac{Q_j^2}{2\varepsilon_0 d_Y}, \quad (47)$$

Hence, the coefficients in the Ising model are given

$$J_j = \frac{2\mathcal{E}_0 - \mathcal{E}_+ - \mathcal{E}_-}{4} = -\frac{2dQ_j^2 X_0^2}{\varepsilon_0 d_Y X_{\text{cap}} (X_{\text{cap}}^2 - 4X_0^2)}, \quad (48)$$

$$B_j = -B_{j+1} = \frac{\mathcal{E}_+ - \mathcal{E}_-}{4} = \frac{dQ_j^2 X_0}{\varepsilon_0 d_Y (X_{\text{cap}}^2 - 4X_0^2)}, \quad (49)$$

$$E_0 = \frac{2\mathcal{E}_0 + \mathcal{E}_+ + \mathcal{E}_-}{4} = \frac{2dQ_j^2 (X_{\text{cap}}^2 - X_0^2)}{\varepsilon_0 d_Y X_{\text{cap}} (X_{\text{cap}}^2 - 4X_0^2)}. \quad (50)$$

Consequently, it is possible to construct an Ising machine based on the comb-teeth MEMS based on the constant-charge condition.

We note that the dynamics is identical between the parallel plates under the constant voltage and the comb-teeth MEMS under the constant charge by suitably changing variables. Namely, there is a kind of duality between the two systems.

A comment is in order. For the sake of completeness, we consider the comb-teeth MEMS under the constant-voltage condition. It follows that

$$\mathcal{E}_0 = \frac{\varepsilon_0 d_Y (X_{\text{cap}} + X_0 - X_0) V_j^2}{d_Z} \frac{1}{2} = \frac{\varepsilon_0 d_Y X_{\text{cap}} V_j^2}{d_Z} \frac{1}{2}, \quad (51)$$

$$\mathcal{E}_{\pm} = \frac{\varepsilon_0 d_Y (d_Y \mp 2X_0) V_j^2}{d_Z}. \quad (52)$$

instead of Eqs.(46) and (47). The coefficients in the Ising model are given by

$$J_j = 0, \quad E_0 = \frac{\varepsilon_0 d_Y X_{\text{cap}} V_j^2}{d_Z} \frac{1}{2}, \quad (53)$$

$$B_j = -B_{j+1} = -\frac{\varepsilon_0 d_Y X_0 V_j^2}{d_Z} \frac{1}{2}, \quad (54)$$

instead of Eqs.(48), (49) and (50). There is no exchange interaction term J_j in this case. Hence, it is impossible to construct a Ising machine by the comb-teeth MEMS.

VI. DUALITY

We have shown that the Ising machine may be constructed with the use of the parallel MEMS under the constant-voltage condition but not under the constant-charge condition. We have also shown that the Ising machine may be constructed with the use of the comb-teeth MEMS under the constant-charge condition but not under the constant-voltage condition.

We now argue that these properties are the consequence of the duality relation.

The differences between two types of MEMS are the electrostatic potentials Eq.(14) under the constant voltage and Eq.(45) under the constant charge, i.e.,

$$U_{\text{para}} = \sum_j \frac{C_{\text{para}}(u_j, u_{j+1})}{2} V_j^2, \quad (55)$$

$$U_{\text{comb}} = \sum_j \frac{Q_j^2}{2C_{\text{comb}}(u_j, u_{j+1})}. \quad (56)$$

They are explicitly given by

$$U_{\text{para}} = \frac{\varepsilon_0 S}{X_{\text{cap}} + u_j - u_{j+1}} \frac{V_j^2}{2}, \quad (57)$$

$$U_{\text{cap}} = \frac{d_Z}{\varepsilon_0 d_Y (X_{\text{cap}} + u_j - u_{j+1})} \frac{Q_j^2}{2}. \quad (58)$$

These two potentials are transformed into one another by

$$V_j \Leftrightarrow Q_j, \quad \varepsilon_0 S \Leftrightarrow \frac{d_Z}{\varepsilon_0 d_Y}. \quad (59)$$

This is the duality relation between the parallel-plate MEMS and the comb-teeth MEMS.

Consequently, all numerical results of the parallel-plate MEMS are applicable to the comb-teeth MEMS by changing parameters according to Eq.(59).

VII. DISCUSSION

First, we proposed nonvolatile memories based on MEMS. In general, it is quite difficult to construct nonvolatile memories only with the use of electric circuits. Spintronics have been employed based on magnetic structure in this context. On the other hand, our method provides us with another possibility to realize nonvolatile memories, which is well compatible with electric circuits. Our results will be useful for memory devices in electric circuits.

Then, we studied an application of MEMS to an Ising machine. In general, temperature is controlled in classical annealing, while external magnetic field is controlled in quantum annealing. They are set above the critical values in the initial stage. Then, they are gradually decreased, during which the annealing occurs. On the other hand, we control external voltage in the annealing method based on the parallel-plate MEMS. In the first step of the annealing process, we keep a constant voltage for a certain period. The essential part of the annealing is over due to the Rayleigh dissipation term. Although we gradually decrease the voltage, this is just to rescale the position to $u_j = \pm X_0$. Thus, the annealing process is quite different from the standard ones. Similar analysis is applicable to the comb-teeth MEMS by controlling the external charge. We would like to point out that the control of the voltage or the charge is easier than the control of the temperature or the magnetic field, which will be of benefit to future applications.

M. E. is very much grateful to E. Saito and N. Nagaosa for helpful discussions on the subject. Y. M. is supported by CREST, JST (JPMJCR20T2). M. E. is supported by

the Grants-in-Aid for Scientific Research from MEXT KAKENHI (Grants No. JP17K05490 and No. JP18H03676) and CREST, JST (JPMJCR16F1 and JPMJCR20T2).

-
- ¹ A. Lucas, *Frontiers in Physics* **2**, 5 (2014)
- ² S. Kirkpatrick, Jr. C. D. Gelatt, M. P. Vecchi, *Science* **220**, 671 (1983).
- ³ V. Cerny, *J. Opt. Theory and Applications* **45** 41 (1985)
- ⁴ T. Kadowaki and H. Nishimori, *Phys. Rev. E* **58**, 5355 (1998)
- ⁵ E. Farhi, J. Goldstone, S. Gutmann, J. Lapan, A. Ludgren and D. Preda, *Science* **292**, 472 (2001)
- ⁶ M. W. Johnson, M. H. S. Amin, G. Rose, *Nature* **473**, 194 (2011)
- ⁷ S. Utsunomiya, K. Takata and Y. Yamamoto, *Opt. Express* **19**, 18091 (2011).
- ⁸ Z. Wang, A. Marandi, K. Wen, R. L. Byer and Y. Yamamoto, *Phys. Rev. A* **88**, 063853 (2013).
- ⁹ A. Marandi, Z. Wang, K. Takata, R. L. Byer and Y. Yamamoto, *Nature Photonics* **8**, 937 (2014).
- ¹⁰ T. Inagaki, Y. Haribara, K. Igarashi, T. Sonobe, S. Tamate, T. Honjo, A. Marandi, P. L. McMahon, T. Umeki, K. Enbutsu, O. Tadanaga, H. Takenouchi, K. Aihara, K.-i. Kawarabayashi, K. Inoue, S. Utsunomiya, H. Takesue, *Science* **354** 603 (2016)
- ¹¹ F. Bohm, G. Verschaffelt and G. V. der Sande, *Nat. Com* **10**, 3538 (2019)
- ¹² H. Goto, *Sci. Rep.* **6**, 21686 (2016)
- ¹³ H. Goto, *J. Phys. Soc. Jpn.* **88**, 061015 (2019)
- ¹⁴ W. A. Borders, A. Z. Pervaiz, S. Fukami, K. Y. Camsari, H. Ohno, and S. Datta, *Nature* **573**, 390 (2019)
- ¹⁵ K. Y. Camsari, S. Chowdhury and S. Datta, *Phys. Rev. Applied* **12**, 034061 (2019)
- ¹⁶ K. Y. Camsari, B. M. Sutton and S. Datta, *Applied Physics Reviews* **6**, 011305 (2019)
- ¹⁷ A. Z. Pervaiz, B. M. Sutton, L. A. Ghantasala and K. Y. Camsari, *IEEE Transactions on Neural Networks and Learning Systems* **30** 1920 (2019)
- ¹⁸ K. Y. Camsari, M. M. Torunbalci, W. A. Borders, H. Ohno and S. Fukami *Phys. Rev. Applied* **15**, 044049 (2021)
- ¹⁹ Y. Mita, A. Hirakawa, B. Stefanelli, I. Mori, Y. Okamoto, S. Morishita, M. Kubota, E. Lebrasseur, A. Kaiser, *Japanese Journal of Applied Physics* **57**, 04FA05 (2018)
- ²⁰ R. Reddy, K. Komeda, Y. Okamoto, E. Lebrasseur, A. Higo, Y. Mita, *Sensors and Actuators A: Physical*, **295**, 1 (2019)
- ²¹ M. Ezawa, *Phys. Rev. B* **103**, 155425 (2021)
- ²² Y. Mita, E. Lebrasseur, M. Ezawa, K. Tsuji, M. Kawamura and A. Higo, "TopoMEMS circuit: step-variable-resettable MEMS capacitor for topological electrical circuit", The 21st International Conference on Solid-State Sensors, Actuators, and Microsystems (Transducers), 20-25 June 2021, online, accepted for publication (2021).